Directed assembly of carbon nanotubes on soft substrates for use as a flexible biosensor array

2008 Nanotechnology 19 505502

(http://iopscience.iop.org/0957-4484/19/50/505502)

Nanotechnology **19** (2008) 505502 (5pp) doi:10.1088/0957-4484/19/50/505502

Directed assembly of carbon nanotubes on soft substrates for use as a flexible biosensor array

Juntae Koh[1], Mihye Yi[2], Byung Yang Lee[1], Tae Hyun Kim[1], Joohyung Lee[1], Young Min Jhon[3] and Seunghun Hong[1]

[1] Department of Physics and Astronomy, Seoul National University, Seoul 151-747, Korea
[2] Korea Research Institute of Chemical Technology, Daejeon 305-343, Korea
[3] Korea Institute of Science and Technology, Seoul 136-791, Korea

E-mail: shong@phya.snu.ac.kr

Received 30 July 2008, in final form 19 October 2008
Published 24 November 2008
Online at stacks.iop.org/Nano/19/505502

Abstract
We have developed a method to selectively assemble and align carbon nanotubes (CNTs) on soft substrates for use as flexible biosensors. In this strategy, a thin oxide layer was deposited on soft substrates via low temperature plasma enhanced chemical vapor deposition, and a *linker-free assembly process* was applied on the oxide surface where the assembly of carbon nanotubes was guided by methyl-terminated molecular patterns on the oxide surface. The electrical characterization of the fabricated CNT devices exhibited a typical p-type gating effect and $1/f$ noise behavior. The bare oxide regions near CNTs were functionalized with glutamate oxidase to fabricate selective biosensors to detect two forms of glutamate substances existing in different situations: L-glutamic acid, a neurotransmitting material, and monosodium glutamate, a food additive.

S Supplementary data are available from stacks.iop.org/Nano/19/505502

(Some figures in this article are in colour only in the electronic version)

Single-walled carbon nanotubes (swCNTs) have been drawing attention for various applications such as field effect transistors (FETs), chemical sensors, and biosensors [1–14]. Although previous reports have shown several methods with which to assemble devices based on CNTs and nanowires (NWs), their applications have usually been limited to solid state substrates [15–18]. On the other hand, the methods to fabricate CNT/NW-based devices on flexible substrates have relied on unconventional fabrication processes which are not compatible with current microfabrication processes [19–27]. Herein, we developed a large scale assembly method of swCNTs onto specific regions of *flexible substrates* with precise orientation for flexible biosensor applications. In this strategy, a thin oxide layer was deposited on soft substrates via low temperature plasma enhanced chemical vapor deposition, and a *linker-free assembly process* [28] was applied on the oxide surface where the assembly of CNTs was guided by methyl-terminated molecular patterns on the oxide surface. Furthermore, we functionalized the swCNT devices to fabricate biosensors to detect two different forms of glutamate substances in different situations: *L-glutamate*, a neurotransmitting material, and *monosodium glutamate (MSG)*, a food additive. Significantly, since the assembly process relies only on conventional microfabrication facilities and allows us to fabricate general swCNT-based device structures on flexible substrates, it should be easily accessible to conventional device industries for various applications such as flexible electronics and sensors.

Figure 1 shows the schematic diagram depicting the basic concepts of our fabrication method. First, a polyimide (PI) precursor prepared from 4,4′-diaminodiphenylether (DDE) and pyromellitic dianhydride (PMDA) diluted by *N*-methyl-2-pyrrolidine (NMP) at the concentration of 20% was coated on a silicon oxide/silicon wafer to the thickness of about 50–60 μm via spin coating at the speed of 1000 rpm for 1 min, and then it was cured on a hot plate in N_2 gas environment (figure 1(A)). For the curing process, the temperature of the hot plate was ramped from 120 to 250 °C with a ramping rate of 5 °C min^{-1}, and then the temperature was sustained at the

final temperature for 1 h. Afterward, a silicon oxide layer with thickness of 200 nm was deposited on the PI layer via plasma enhanced chemical vapor deposition at 150 °C (figure 1(B)). This SiO_2 layer worked as a buffer layer for molecular patterning and swCNT adsorption. The molecular patterning and selective swCNT process on the SiO_2 layer was similar to that reported previously (figure 1(C)) [28–30]. Briefly, AZ5214 photoresist was first patterned via photolithography, and the substrate was dipped in octadecyltrichlorosilane (OTS) solution (OTS:hexane = 1:500 v/v) for 10 min at a temperature of 23 °C and humidity of 80%. Then, the substrate was rinsed with clean anhydrous hexane, acetone and ethanol, followed by heating in a convection oven at a temperature of 50 °C for 10 min to enhance OTS functionalization on the oxide layer. When the sample was dipped in an swCNT suspension (0.05 mg ml^{-1} in *o*-dichlorobenzene) for ∼5 s, swCNTs were selectively adsorbed and aligned on the bare SiO_2 surface regions. Source and drain electrodes were patterned by photolithography and thermally deposited with Pd (thickness ∼20 nm) followed by a lift-off process (figure 1(D)). It should be noted that the entire process including molecular patterning could be performed using conventional microfabrication facilities.

The fabricated swCNT junctions were functionalized with glutamate oxidase to fabricate biosensors to detect glutamate (figure 1(E)). In this process, the bare SiO_2 surface between swCNTs was first functionalized with amine functional groups by dipping the swCNT junctions in 3-aminopropyltriethoxysilane (APTES) solution (1:500 v/v in ethanol) for 20 min. Then, the sample was dipped in an aqueous solution of glutaraldehyde (1:20 v/v in deionized (DI) water) for 1 h and then in the glutamate oxidase solution (a few mg in 20 μl PBS (phosphate buffered saline) solution of pH 7.4 and 10 mM) for 12 h. Here, glutaraldehyde molecules worked as a linker to connect the amine groups on the substrate and that on the glutamate oxidase molecules (figure S1 in the supporting information available at stacks.iop.org/Nano/19/505502). For sensing experiments, PBS solution was first applied on the swCNT-based biosensor (figure 1(F)). Here, 0.01 V was applied between the source–drain electrodes, while the platinum liquid gate was grounded. Then, the solution of a specific glutamate was added resulting in certain concentration, while monitoring the change of current levels using a semiconductor parameter analyzer (Keithley 4200).

Figure 2(A) shows a typical swCNT pattern where CNTs were adsorbed onto 4 μm wide bare SiO_2 regions between 2 μm wide regions of an OTS self-assembled monolayer (SAM) [28–30]. The swCNTs were selectively adsorbed onto the polar SiO_2 surfaces while the OTS SAM prevented the swCNT adsorption. It should be noted that the swCNT patterns had well-defined boundaries without any crossing of swCNTs. This result indicates that one can use the directed assembly process to assemble and align swCNTs on flexible substrates.

Figure 2(B) shows the adsorbed amount of swCNTs on polar regions depending on the dipping time in the swCNT suspensions [31]. The adsorbed swCNT density rapidly increased within the first 100 s and reached a saturation value

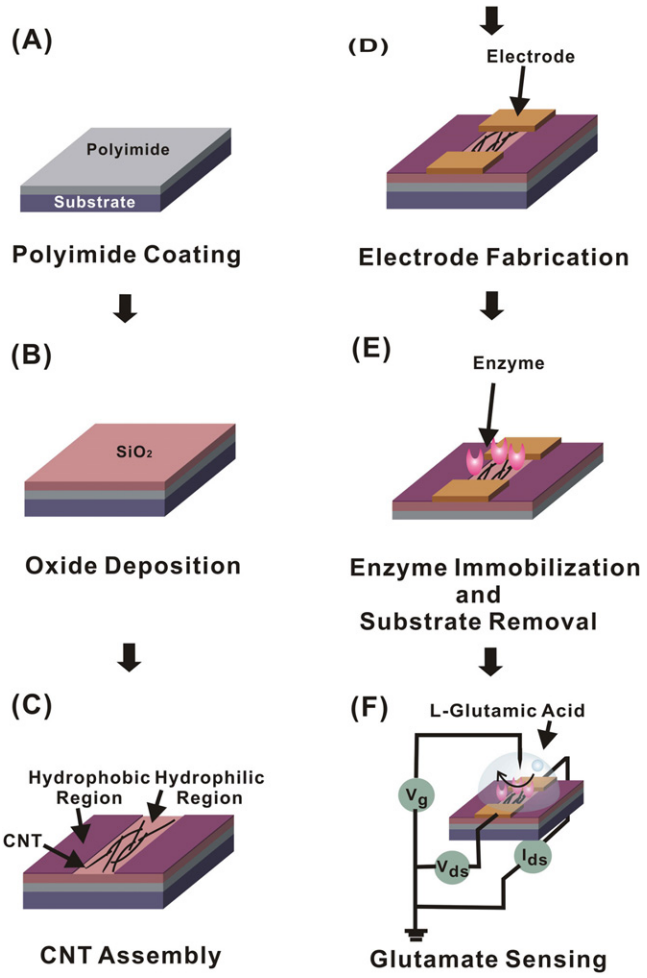

Figure 1. Schematic diagram depicting the fabrication of single-walled carbon-nanotube-based flexible biosensors.

after ∼100 s, which is similar to the adsorption behavior of Langmuir isotherm processes. In the Langmuir isotherm process, as the adsorbate molecules get adsorbed to the binding sites on the solid substrates, they passivate the binding sites and prevent additional adsorption. Thus, after a while, the density of adsorbates reaches a saturated density due to equilibrium between the association and dissociation processes. The graph can be fitted by the equation for the Langmuir isotherm as follows.

$$\theta(t) = \theta_0 \frac{C}{C + (k_d/k_a)}[1 - \exp((-k_a C + k_d)t)] \quad (1)$$

where θ_0, C, k_a, and k_d are the maximum surface density of adsorbed swCNTs, the concentration of swCNTs solution, association coefficient, and dissociation coefficient, respectively [32]. Since the concentration ($C \sim 0.05$ mg ml^{-1}) of the swCNT solution is known, we can determine the other parameters by the fitting. The maximum surface density θ_0 of adsorbed swCNTs is 3.5539 μm^{-2}, the association coefficient k_a is 1.9208 ml mg^{-1} s^{-1}, and the dissociation coefficient k_d is 6.0×10^{-5} s^{-1}. The results show that $Ck_a \gg k_d$, indicating that the swCNT adsorption from the solution, rather than dissociation from the substrate, was the dominating factor determining our assembly process.

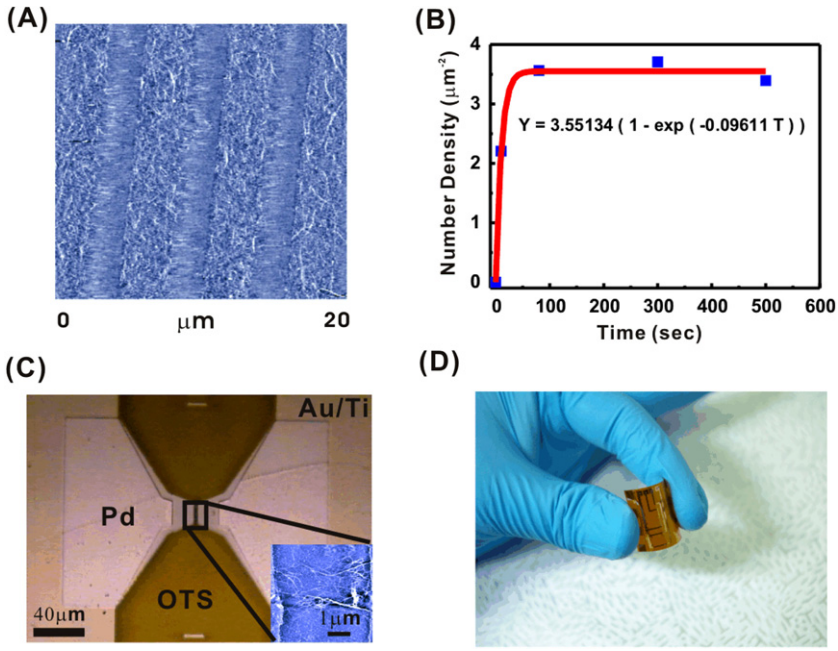

Figure 2. The swCNT adsorption properties and swCNT-based flexible devices. (A) Line-shape patterns comprised of adsorbed swCNTs (line width ∼4 μm) and OTS passivation regions (line width ∼2 μm). (B) Adsorption data (square dots) of swCNTs onto a 4 × 4 μm^2 region on the SiO_2/PI surface and the theoretical fitting (red line) based on the Langmuir isotherm. (C) Optical micrograph of an swCNT device. The inset shows the AFM image of swCNT patterns between the electrodes. (D) Optical image of a fabricated flexible biosensor.

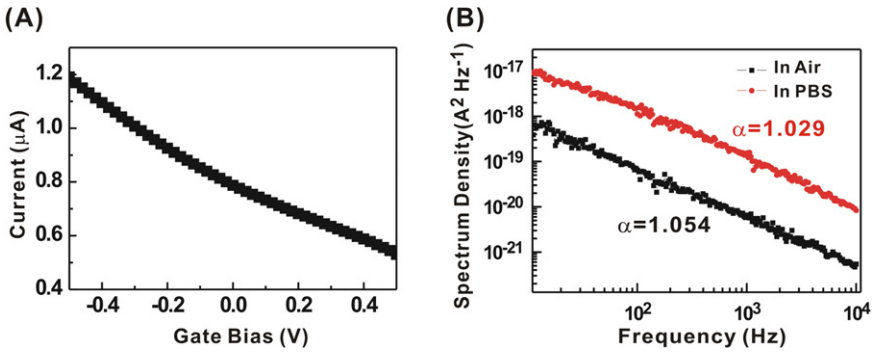

Figure 3. Electrical properties of the fabricated swCNT devices on flexible substrates. (A) A typical liquid gate property of an swCNT junction immersed in the PBS solution. The Pt liquid gate was swept from −0.5 to 0.5 V with a source–drain bias of 0.01 V. (B) Noise spectrum density of a flexible swCNT device with a source–drain bias of 1 V.

Since the adsorbed swCNTs formed stable structures, we could continue additional microfabrication processes to build swCNT-based devices (figure 2(C)). Here, a Pd layer was first patterned to achieve low contact resistance with the swCNTs [33]. However, since the Pd layer did not adhere to the SiO_2 well, it was not suitable for a long interconnection on flexible substrates. We fabricated additional Au/Ti electrodes for the long interconnections to measurement instruments. The fabricated devices did not exhibit any change of electrical properties even when they were bent with a radius of curvature down to 0.5 cm (figure 2(D)).

Figure 3(A) shows a typical liquid gating effect of swCNT junctions using a Pt reference electrode as a liquid gate in PBS solution. Cyclic gate sweeping between −0.5 and 0.5 V was applied five times with $V_{ds} = 0.01$ V, and the results were averaged for the five cycles, resulting in typical p-type FET behavior. The threshold voltage was estimated as ∼1.3 V via linear extrapolation, and the transconductance of this device was ∼0.63 μA V^{-1}. This device did not turn off completely because the network consisted of a percolated network of metallic and semiconducting swCNTs. It should be noted that the self-limiting adsorption behavior of swCNTs (figure 2(B)) allows us to prepare rather uniform-density swCNT networks for our devices, which enhances the reproducibility of our fabrication method compared with previous FET devices comprised of a single swCNT [28]. Furthermore, we could fabricate devices exhibiting rather uniform responses to the same analyte (figure S2 in the supporting information available at stacks.iop.org/Nano/19/505502).

The noise characteristics of the device in the conditions of exposure to air and PBS buffer solution were measured using a fast Fourier transform analyzer (HP 3562A). The gate for the junction exposed to air was floated, while the liquid gate (platinum electrode) was grounded for the junctions in the PBS

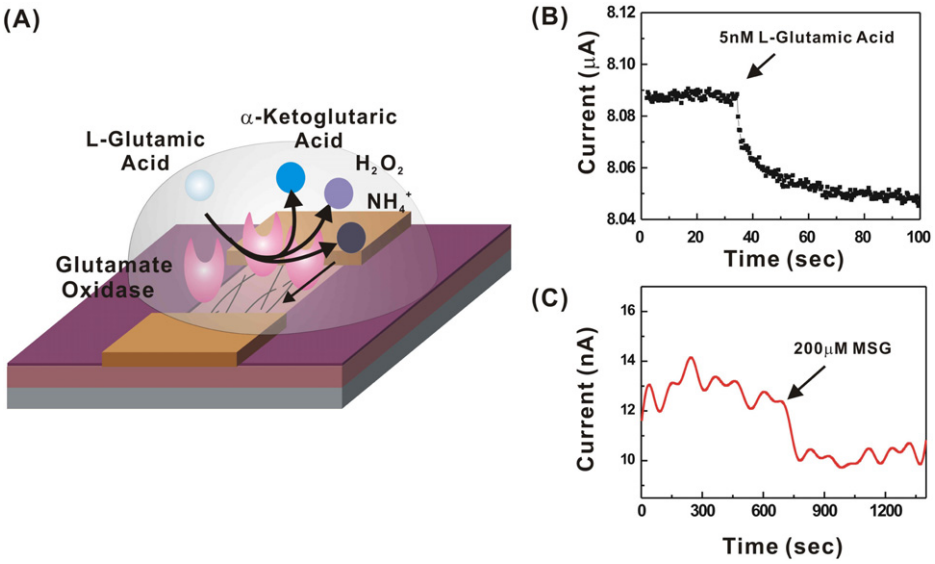

Figure 4. Detection of glutamate. (A) Schematic diagram depicting the proposed detection mechanism. Glutamate oxidase oxidizes the glutamate and generates various by-products. One of the by-products, ammonia, is expected to reduce the conductance of the swCNT junctions. (B) Detection of 5 nM L-glutamate using our flexible biosensor with a source–drain bias of 0.01 V and a source–gate bias of 0 V. (C) Detection of 200 μM MSG using our flexible biosensor with a source–drain bias of 0.1 V and a source–gate bias of 0 V.

buffer solution. 1 V was applied between the source and drain electrodes for both cases. Figure 3(B) shows that the junction exposed to buffer solution exhibits higher noise level than the one exposed to air. The Hooge model is generally used as the empirical description of noise phenomena by the following formula:

$$S_I = A\frac{I^2}{f^\alpha}. \tag{2}$$

Here, A and α were determined by fitting the noise power spectrum in a log–log scale using equation (2). α was estimated to be 1.054 and 1.029 for two different junctions, which indicated a typical $1/f$ noise behavior as reported before [34–37]. A was estimated to be about 1.949×10^{-5} and 1.722×10^{-4} for the junction exposed to air (resistance $R \sim 1.472 \times 10^6\ \Omega$) and buffer solution ($R \sim 1.087 \times 10^6\ \Omega$), respectively. Previous reports show that $A/R \sim 10^{-11}$ for CNT devices with the junction exposed to air [38]. In our case, A/R is 1.324×10^{-11} and 1.584×10^{-10} for air and liquid environments, respectively. This indicates that our flexible biosensors in air have comparable noise levels to swCNT devices on solid substrates. The increased noise level in PBS solution was also expected due to the liquid environment.

Flexible biosensors based on swCNTs were fabricated by functionalizing the bare SiO_2 regions between swCNTs in the device with glutamate oxidase (figure S1 in the supporting information available at stacks.iop.org/Nano/19/505502). When the glutamate is injected, the glutamate oxidase oxidizes the glutamate molecules and generates several by-products (figure 4(A)). One of the by-products, ammonia, was expected to reduce the conductance of the swCNT junctions [4]. We performed extensive control experiments on the effect of all by-products (α-ketoglutaric acid, ammonia, and hydrogen peroxide) on our swCNT junctions, and reproducibly found that only ammonia significantly reduced the conductance of our swCNT junctions (figure S3 in the supporting information available at stacks.iop.org/Nano/19/505502). The results support our explanation that the sensing signals of our glutamate sensors came from the ammonia generated by the enzymatic reaction. This biosensor can be used to detect two different forms of glutamate substances existing in different situations: L-glutamate and MSG. It also should be noted that since the enzyme functions properly only around physiological pH conditions (∼pH 7.4), we cannot use our sensors in highly acidic or basic solutions (figure S4 in the supporting information available at stacks.iop.org/Nano/19/505502).

L-glutamate is a neurotransmitting material between neuron cells. The detection of glutamate could be extremely important for various applications such as monitoring patient conditions during brain surgery [39]. Figure 4(B) shows the response of our biosensor to 5 nM L-glutamate. Here, the glutamate enzyme fixed on the swCNT devices oxidized L-glutamate, and one of the by-products in this reaction, ammonia, changed the conductance of the devices.

The fabricated biosensors also can be utilized to detect another form of glutamate, MSG. MSG is a well-known food additive which often causes allergic reactions (called 'MSG symptom complex') in some people. MSG exists mostly in food, while L-glutamate is most abundant between neuronal networks. Since the two substances exist in quite different environments, we can use our biosensors for the selective detection of both substances. Figure 4(C) shows the response to 200 μM MSG solution. Previous research shows that the concentration of MSG in typical processed food is 0.2–0.9%, which corresponds to 19–86 mM concentration [40]. The result in figure 4(C) implies that our sensors have a high enough sensitivity for the detection of MSG in typical processed food. We demonstrated the application of our sensors to some real food samples, rice

soup (figure S5 in the supporting information available at stacks.iop.org/Nano/19/505502). However, one should be cautious in applying our glutamate sensors to general real samples because many real samples such as blood and foods may contain extremely diverse chemical species whose effects on our devices are yet to be explored.

In summary, we utilized molecular patterns to selectively assemble and align swCNTs onto flexible substrates and demonstrated the fabrication of swCNT-based flexible biosensors. The fabricated swCNT devices exhibited typical p-type transistor characteristics in PBS solution and a noise level comparable to that on solid substrates. As a proof of concept, swCNT devices were functionalized with glutamate oxidase to fabricate flexible biosensors to detect two forms of glutamate substances existing in different environments: (1) L-glutamate, a neurotransmitting material between neurons, and (2) MSG, a food additive. Since this fabrication method utilizes only conventional microfabrication facilities, it should be readily accessible to present industries for the mass production of flexible biosensors for various applications such as the monitoring of neuro-activity and the detection of food additives.

Acknowledgments

The work was supported by an NRL grant (No. R0A-2004-000-10438-0) funded by the Korea Science and Engineering Foundation (KOSEF) and Seoul R&DB program (GR070045). SH acknowledges the partial support from the Eco-technopia 21 project by Korea Ministry of Environment. The research at KRICT was financially supported by a grant from the Fundamental R&D Program for Core Technology of Materials funded by the Ministry of Knowledge and Economy. YMJ and SH are grateful for the support through the 'System IC 2010' Project of Korea Ministry of Knowledge Economy.

References

[1] Iijima S 1991 *Nature* **354** 56
[2] Chen Z H, Appenzeller J, Lin Y M, Sippel-Oakley J, Rinzler A G, Tang J Y, Wind S J, Solomon P M and Avouris P 2006 *Science* **311** 1735
[3] Ghosh S, Sood A K and Kumar N 2003 *Science* **299** 1042
[4] Kong J, Franklin N R, Zhou C W, Chapline M G, Peng S, Cho K J and Dai H J 2000 *Science* **287** 622
[5] Tans S J, Devoret M H, Dai H J, Thess A, Smalley R E, Geerligs L J and Dekker C 1997 *Nature* **386** 474
[6] Javey A, Guo J, Farmer D B, Wang Q, Wang D W, Gordon R G, Lundstrom M and Dai H J 2004 *Nano Lett.* **4** 447
[7] Avouris P, Chen Z H and Perebeinos V 2007 *Nat. Nanotechnol.* **2** 605
[8] Lee A C, Ye J S, Tan S N, Poenar D P, Sheu F S, Heng C K and Lim T M 2007 *Nanotechnology* **18** 455102
[9] Valentini L, Armentano I, Kenny J M, Cantalini C, Lozzi L and Santucci S 2003 *Appl. Phys. Lett.* **82** 961
[10] Someya T, Small J, Kim P, Nuckolls C and Yardley J T 2003 *Nano Lett.* **3** 877
[11] Koehne J, Chen H, Li J, Cassell A M, Ye Q, Ng H T, Han J and Meyyappan M 2003 *Nanotechnology* **14** 1239
[12] Besteman K, Lee J O, Wiertz F G M, Heering H A and Dekker C 2003 *Nano Lett.* **3** 727
[13] Modi A, Koratkar N, Lass E, Wei B Q and Ajayan P M 2003 *Nature* **424** 171
[14] Snow E S, Perkins F K, Houser E J, Badescu S C and Reinecke T L 2005 *Science* **307** 1942
[15] Wang Y H, Maspoch D, Zou S L, Schatz G C, Smalley R E and Mirkin C A 2006 *Proc. Natl Acad. Sci. USA* **103** 2026
[16] Krupke R, Hennrich F, von Lohneysen H and Kappes M M 2003 *Science* **301** 344
[17] Huang Y, Duan X F, Wei Q Q and Lieber C M 2001 *Science* **291** 630
[18] Kong J, Soh H T, Cassell A M, Quate C F and Dai H J 1998 *Nature* **395** 878
[19] Kang S J, Kocabas C, Kim H S, Cao Q, Meitl M A, Khang D Y and Rogers J A 2007 *Nano Lett.* **7** 3343
[20] Meitl M A, Zhou Y X, Gaur A, Jeon S, Usrey M L, Strano M S and Rogers J A 2004 *Nano Lett.* **4** 1643
[21] Park J-U, Meitl M A, Hur S-H, Usrey M L, Strano M S, Kenis P J A and Rogers J A 2005 *Angew. Chem. Int. Edn* **45** 581
[22] Maune H and Bockrath M 2006 *Appl. Phys. Lett.* **89** 173131
[23] Sun Y and Wang H H 2007 *Adv. Mater.* **19** 2818
[24] Sun Y and Wang H H 2007 *Appl. Phys. Lett.* **90** 213107
[25] Kang S J, Kocabas C, Ozel T, Shim M, Pimparkar N, Alam M A, Rotkin S V and Rogers J A 2007 *Nat. Nanotechnol.* **2** 230
[26] Bradley K, Gabriel J C P and Gruner G 2003 *Nano Lett.* **3** 1353
[27] Kang J, Lee J, Kim T H, Park J, Seong M J and Hong S 2008 *Nanotechnology* **19** 135305
[28] Lee M, Im J, Lee B Y, Myung S, Kang J, Huang L, Kwon Y K and Hong S 2006 *Nat Nanotechnol.* **1** 66
[29] Rao S G, Huang L, Setyawan W and Hong S H 2003 *Nature* **425** 36
[30] Myung S, Lee M, Kim G T, Ha J S and Hong S 2005 *Adv. Mater.* **17** 2361
[31] Im J, Huang L, Kang J, Lee M, Lee D J, Rao S G, Lee N K and Hong S 2006 *J. Chem. Phys.* **124** 224707
[32] Karpovich D S and Blanchard G J 1994 *Langmuir* **10** 3315
[33] Javey A, Guo J, Wang Q, Lundstrom M and Dai H J 2003 *Nature* **424** 654
[34] Soliveres S, Gyani J, Delseny C, Hoffmann A and Pascal F 2007 *Appl. Phys. Lett.* **90** 082107
[35] Briman M, Bradley K and Gruner G 2006 *J. Appl. Phys.* **100** 013505
[36] Reza S, Huynh Q T, Bosman G, Sippel-Oakley J and Rinzler A G 2006 *J. Appl. Phys.* **99** 114309
[37] Dutta P and Horn P M 1981 *Rev. Mod. Phys.* **53** 497
[38] Snow E S, Novak J P, Lay M D and Perkins F K 2004 *Appl. Phys. Lett.* **85** 4172
[39] Hillered L, Persson L, Ponten U and Ungerstedt U 1990 *Acta Neurochir.* **102** 91
[40] Rundlett K L and Armstrong D W 1994 *Chirality* **6** 277